International Journal on Advanced Science Engineering Information Technology

Vol.10 (2020) No. 6
ISSN: 2088-5334

Finite Element Numeric Simulation of Organic Solar Cells with Gold Thin Film

Grazia Lo Sciuto[a,1], Salvatore Coco[a], Dor Gotleyb[b], Rafi Shikler[b,1]

[a]*Department of Electrical, Electronics and Informatics Engineering, University of Catania, Viale Andrea Doria 6, Catania, 95125, Italy*
E-mail: [1]glosciuto@dii.unict.it

[b]*Department of Electrical and Computer Engineering, Ben-Gurion University of the Negev, P. O. B. 653 Beer-Sheva, Israel*
E-mail: [1]rshikler@bgu.ac.il

***Abstract*— In this paper, we have explored the potential of organic solar cells with gold layers, simulating different geometries and comparing them with the experimental data obtained from the devices produced at the "optoelectronic organic devices laboratory at Ben Gurion University of the Negev, Israel." Thin-film heterojunction solar devices are analyzed using a basic chemical technology of GLASS/ITO/PEDOT,PSS/P3HT, PCBM, and another type of nanostructure where the gold layer is added. A standard device is realized on top of a transparent substrate such as glass or flexible polymer Polyethylene Terephthalate (PET). The first layer is the anode, which is made of conductive material and is also transparent. In our case, the very common material Indium-Tin-Oxide (ITO) is used. To facilitate the transition between the active layer and the anode, an intermediate layer is introduced. Hole Transport Layer (HTL) 's high hole mobility allows holes to move towards the anode instead of the cathode. On top of these layers the organic active layer is constituted by a blend of two organic materials configuring a multiple junction morphology (Bulk Heterojunction or BHJ). In our case, two commonly organic materials [6,6]-Phenyl C61 Butyric acid Methyl ester and Poly(3-Hexylthiophene-2,5-diyl) (PCBM:P3HT) are used. The cathode on top organic active layer is made of highly conductive opaque metal, mostly Aluminum (Al). The finite-element method has been used to compute the electromagnetic field distributions. The results show that the model with the gold layer increases the electrical performance of organic solar cells.**

***Keywords*— power density flow; FEM; organic solar cells.**

I. INTRODUCTION

Power generation by solar cells/modules is a promising renewable energy candidate for future cars. Most EFVs are equipped with large-capacity batteries that can be charged with electricity generated by solar cells/modules. It has been reported that installing 800 W rated solar power modules on automobiles can significantly reduce CO_2 emissions from passenger cars. However, the photovoltaic modules need to be installed on the roof and the side doors, engine hood, and the hatch of passenger cars [1]. Green technology includes urban context services for buildings, public infrastructures, and smart community involving sustainable energy generated from solar panels, wind turbines, and biogas. The challenge of providing the world energy demand is aggravating each year, with billions of people still living without proper electricity access.

The conventional energy sources are still costly and highly polluted. In the last decade, large amounts of money in renewable energies have been invested, which are clean, inexpensive, and suited for various applications [2], [3]. Solar energy is the most popular among alternative green energy sources. Recently, organic solar cells (OSCs) have emerged as an efficient and sustainable energy technology. Their prominent attributes of being lightweight, low-cost, mechanically flexible, and enabling ease of largescale fabrication have attracted even more attention from academia and the industry over the decades [4]. These properties can combine to a low-cost large-area device with an undemanding fabrication process [5]–[10].

OSCs may find application in a host of technologies, ranging from smart windows and skins of future buildings to optical displays, glare-control devices, and rearview mirrors in automotive. A photo-electrochromic device with integrated photovoltaic and electrochromic components enables an adjustable transparency glazing where the photovoltaic part supplies the power to drive the coloration. Such stand-alone, self-powered, wireless devices are of commercial interest for integration into glass windows and surfaces of buildings and automotive or aeronautic vehicles.

These devices with smart window applications can be effectively implemented in modern energy-saving buildings

[11]. Many resources were invested in pursuing better organic materials, fabrication processes, and device configurations. As evidence, the efficiency of a lab OSC has already reached 11% percent. Yet, there is still a need for extensive investigation to exploit the full extent of this technology. The optical transmittance and conductivity for thin metallic films, such as Au, are critical parameters in organic photovoltaics for obtaining an extra-ordinary improvement in the overall solar cell efficiency (to the order of 49%) when the Au thin film transmittance was increased from 38% to 54% [12].

Gold quantum dots (AuQDs) are employed as photosensitizers in organic thin-film solar cells (OSCs) to improve their photoelectric conversion properties. The enhancement in the polymer solar cells efficiency is related to the increase in their absorptivity due to the far-field and near-field effect of localized surface plasmon resonance. It is induced by the presence of the Gold nanorods and introduced by spin-coating their aqueous solution directly on top of poly(3-hexy lthiophene-2,5-diyl):[6,6]-phenyl-C_{61}-butyric-acid methyl ester layer, in the interface between the photoactive layer and the metallic rear electrode [13]. The periodically arranged colloidal gold nanoparticles integrated at the bottom electrode of organic solar cells (OSCs) and light absorption enhancement in the active organic layer are demonstrated experimentally and numerically investigated in bulk hetero-junction solar cells based on the Finite-Difference Time-Domain (FDTD) and Transfer Matrix Method (TMM) [14]–[17].

In this paper, the optical models relative to two organic samples exhibiting the same structure GLASS/ITO/PEDOT: :PSS/P3HT:PCBM are considered. The only difference between the two consists of an addition of gold layers in one of them. The electromagnetic analysis is aimed at evaluating the electric power obtainable. It was conducted using a Finite Element discretization in which the devices behaviour has been simulated on a large range of frequencies. We have referred to the OSCs fabricated in Optoelectronic Organic Semiconductor Devices Laboratory (OOSDL) (see Fig.1).

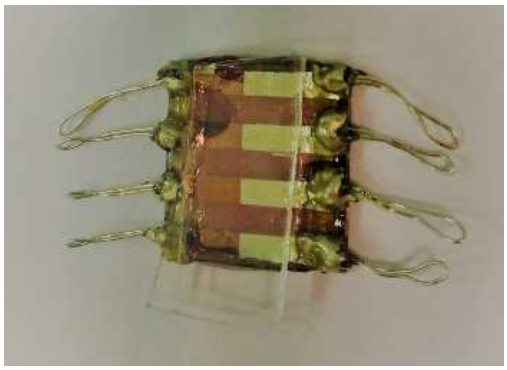

Fig. 1 The manufactured organic solar cell.

The paper is structured as follows: in section II and III, photoelectric materials and fabrication of OSCs are described in details; in section IV, the FE numerical analysis is illustrated; in section V numerical simulations are compared to experimental data. Conclusions are presented in section VI.

II. Material and Method

OSCs are made of sandwiching layers with different functionalities, as shown in Fig. 2. A standard device is realized on top of a transparent substrate such as glass or flexible polymer Polyethylene Terephthalate (PET). The first layer is the anode, which is made of conductive material and is also transparent. In this work, the very com-mon material Indium-Tin-Oxide (ITO) is used. To facilitate the transition between the active layer and the anode, an intermediate layer is introduced. The high hole mobility of the Hole Transport Layer (HTL) allows to holes to move towards the anode instead of the cathode [18]–[20].

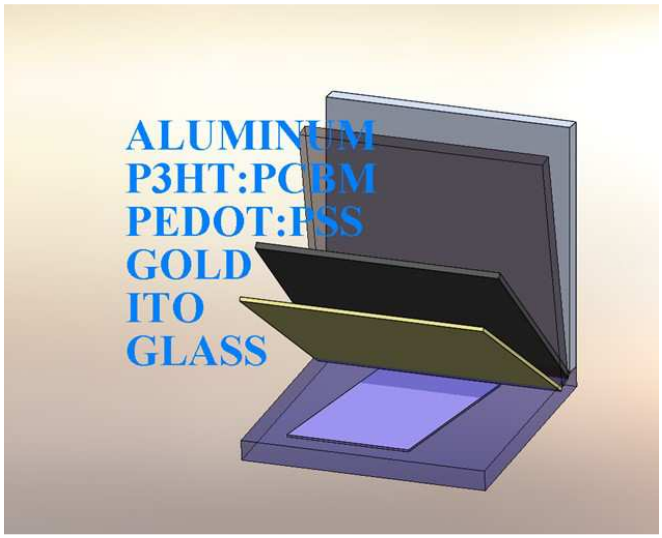

Fig. 2 The typical architecture of a polymer solar cell consists of different layers sandwiched between the anode and the cathode: glass, ITO, gold, PEDOT:PSS, P3HT:PCBM and Aluminium.

These three layers are transparent in order to allow the light to penetrate to the active layer. On top of these layers the organic active layer is constituted by a blend of two organic materials configuring a multiple junction morphology (Bulk Heterojunction or BHJ), in our case two commonly organic materials [6,6]-Phenyl C61 Butyric acid Methyl ester and Poly(3-Hexylthiophene-2,5-diyl) (PCBM:P3HT) are used. The cathode on top organic active layer is made of highly conductive opaque metal, mostly Aluminum (Al). The process of photocurrent generation is shown in Fig. 3.

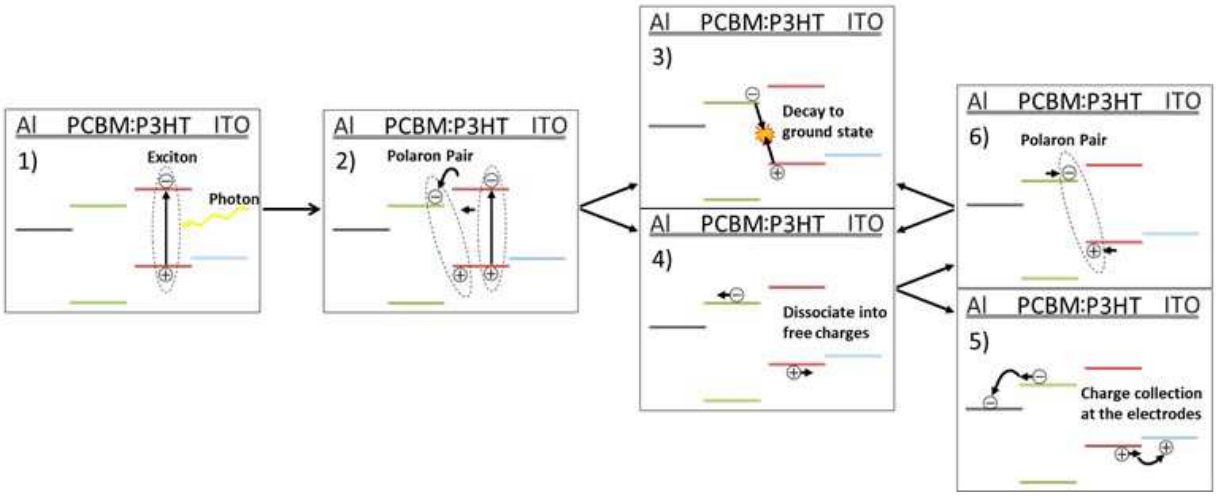

Fig. 3 The processes leading to photocurrent in the BHJ solar cell from the energy diagram's perspective. (1) light absorbs at the P3HT and generates excitons. (2) Excitons diffuse toward the PCBM:P3HT interface. The electron transfers into the PCBM, and a PP state is created. (3,4) The PP decay to ground state or dissociate to free charges with a finite probability. (5) after PP dissociation, the free charges transport towards the electrodes and are being collected, or (6) meet an interface again to reproduce a PP.

The scheme of the four relevant materials band diagram are depected in figure (from left to right): Al (gray line), PCBM (green lines), P3HT (red lines), and ITO (blue line). The Fermi levels indicate the electrodes and organic semiconductors are indicated by two lines. The lower line represents the HOMO (Highest Occupied Molecular Or-bit corresponding to the conduction band in inorganic semiconductors), and the upper line represents the LUMO (Lo-west Unoccupied Molecular Orbit, corresponding to the valence band in inorganic semiconductors).

- Photons absorbed in the organic layer (mainly in the P3HT) generates excitons, a quasi-neutral particle composed of an electron and hole bounded together by Coulomb force. The auxiliary energy for dissociation is provided at the interface of the PCBM:P3HT.
- The excitons are diffusing toward the organic materials interface. The electron transfers into the adjacent molecule, and a second quasi-neutral particle is generated, a Polaron-Pair (PP). The PP is a state of an electron and hole bounded together by weaker coulomb force and probability dissociating to free charges.

Since excitons have a concise diffusion length (few nanometers), efficiently, the carriers dissociate only at the interface of organic materials composed by the active layer. A dense junction layer is required to achieve a BHJ configuration. (3,4) In the next phase, the finite probability for the PP to decay to the ground state or dissociate to free charge carriers depends highly on the internal electric field (Fig. 3). (5) The free charge carriers can then transport via an electric field to electrodes, holes to anode, and electrons to cathode. However, since the device is a BHJ, instead of reaching the electrodes, (6) the free charges can meet with another organic interface to generate again a PP, this process called Back Electron Transport (BET).

This is a closed-loop with a finite probability of collecting the charges and produce electricity. Due to fabrication limitations, the transparent anode slightly spreads out from the actual area of the organic layer to make a place connected to the outer circuit. This additional ITO increases power losses. To avoid this, a gold layer was evaporated right next to the location of cells.

This highly conductive later that has a similar work function to the ITO reduces the transition distance of holes inside the transparent ITO. To examine this configuration, a set of OSCs has been produced. A sample of realized device is shown in Fig. 1. The pro-cess steps are as follows: a 12x12 mm glass coated with an ITO with dimensions of 6x12 mm and a thickness of 90 nm and resistivity of 20 Ω/sq is used as a substrate. The substrate is cleaned in an ultrasonic bath with acetone, methanol, and iso-propanol for 15 min each, after which it is placed in a plasma asher for 4 min. The second stage is the thermal evaporation of 30 nm of gold using the shadow mask shown in Fig. 4.

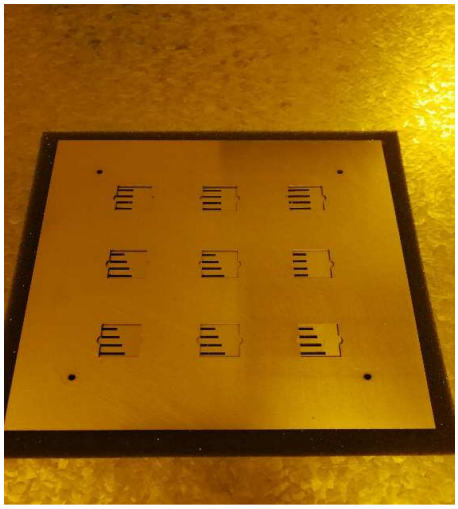

Fig. 4 The shadow mask used to manufacture the solar cell. The mask comprises 9 modules; each module contains 4 fingers in different sizes determining the cells lengths.

The shadow mask was designed in a way that the gold will be well-positioned. The shadow mask consists of 9 modules; each has four strips with a width of 1.5 mm, which

defines one solar cell. Thus, on each substrate, four cells are located. Each module consists of different sets of strip lengths providing different cell lengths, from 1 mm to 6 mm. Following the bottom contact formation, a 30 nm of HTL made of the highly conductive, high transparent polymer poly(3,4 ethylene dioxythiophene) polystyrene sulfonate (PEDOT:PSS) is spin-coated, and the device is dried for 1 hour at high temperature to extract the excessive water.

Afterward, 100 nm of the organic layer (PCBM:P3HT) is spin-coated inside a nitrogen environment to avoid moisture and oxygen exposition. Then, 80 nm of Aluminum is evaporated through the same shadow mask shown in Fig. 4. In this step, the substrate is rotated 180° and placed in the corresponding module to create a continuous strip con-sisted of gold on one side and Al on the other side. To further increase performance, the device is annealed at 140 ° for 20 minutes. To complete the device, eight electric wires are then glued using conductive silver epoxy to the device, one for each electrode. Then, a small piece of glass is glued on top of the device for encapsulation. The following equations govern the electromagnetic field distribution for OSCs:

$$\nabla \times E = -j\omega\mu_0\mu_r H \tag{1}$$

$$\nabla \times H = -j\omega\varepsilon_0\varepsilon_r E \tag{2}$$

Where ω is the angular frequency, μ_0 and ε_0 are the permeability and permittivity of free space, respectively μ_r is the relative permeability and ε_r is the relative permittivity which is assumed to be constant in each material. By combining (1) and (2) the following equation is obtained:

$$\nabla \times \left(\frac{1}{j\omega\mu_r} \nabla \times E \right) - k_0^2 \varepsilon_r E = 0 \tag{3}$$

Where $k^2_0 = \omega^2\varepsilon_0\mu_0$. The physical organic devices derive the three-dimensional models with pe-culiar geometries, and materials are shown in Fig. 5 and Fig. 6. The first model consists of the following layers from the bottom: glass, ITO, PEDOT: PSS layer, PCBM: P3HT, and Aluminum representing the basic components of the solar cell without the encapsulation and protective cover. The component and its arrangement are shown in Fig. 5. The glass substrate is 0.7 mm thick, ITO layer and Aluminum are respectively 90 nm and 80 nm thicks, PCBM: P3HT is 200 nm thick, and PEDOT:PSS is 30nm thick. The aluminum layers are the smallest in size and thus determine the mesh size's slightest extent.

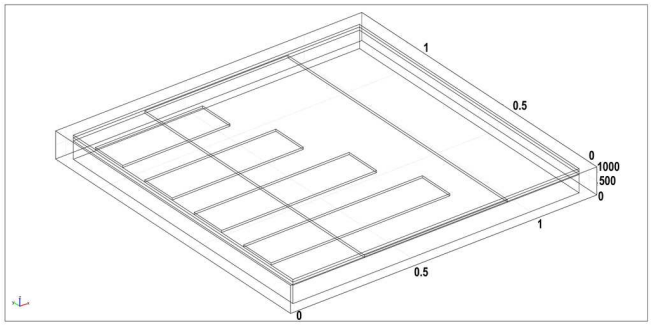

Fig. 5 The structures simulated in COMSOL Multiphysics: geometry of a device without gold layer.

In the second model, the layers are arranged as shown in Fig. 6 with the same basic model configuration, but a 30 nm thick gold layer is added between ITO and PEDOT: PSS. The FE solutions of equation (3) for the two 3D models are carried out using the RF Module of commercial product COMSOL Multiphysics. In the discretization, meshes are used at 2.5 nm length. The model meshes with coarse size mesh on the broader region, and the mesh is finer at the narrow regions such as the interface aluminum and active layers. Absorbing boundary conditions, perfectly matched layer (PML), are used in the simulations.

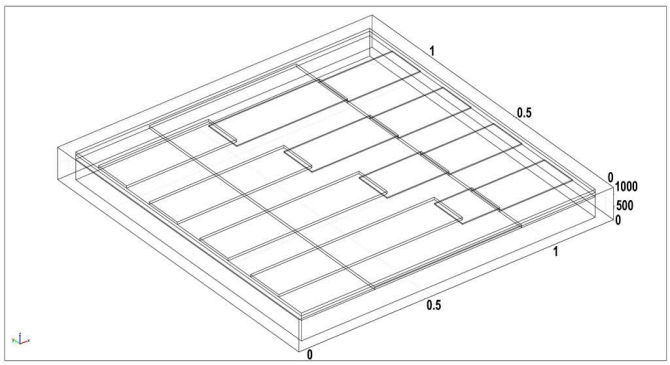

Fig. 6 The structures simulated in COMSOL Multiphysics: geometry of a device with gold layer.

Thin multi-layered structure procures the optical interference effect in each layer having distinct electrical conductivity. For this purpose, the optical and physical properties of organic materials are described by complex wavelength-dependent refraction index (n) and extinction coefficient (k) taken from the literature. For the gold the refractive index and extinction coefficient used in these simulations are: k = 3.5427, n = 0.16541 related to a wavelength of 6.644 µm. To represent the light in the simulations was used as an electric field incident in the device with wavelength ranging from 400 nm to 800 nm (Fig. 7 and Fig. 8).

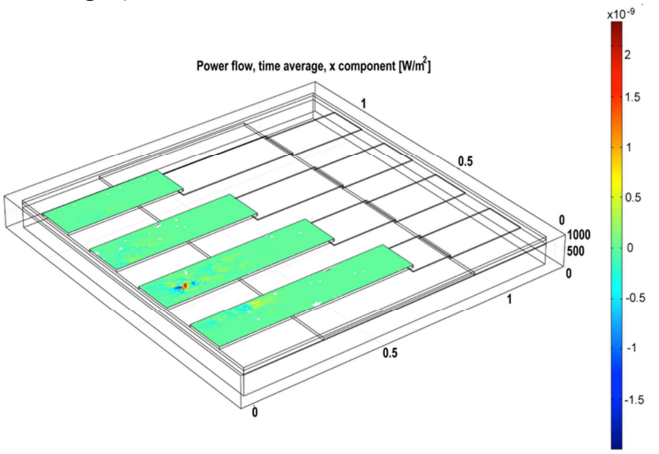

Fig. 7 Power flow, time average, x component [W/m^2] in a device with gold layer.

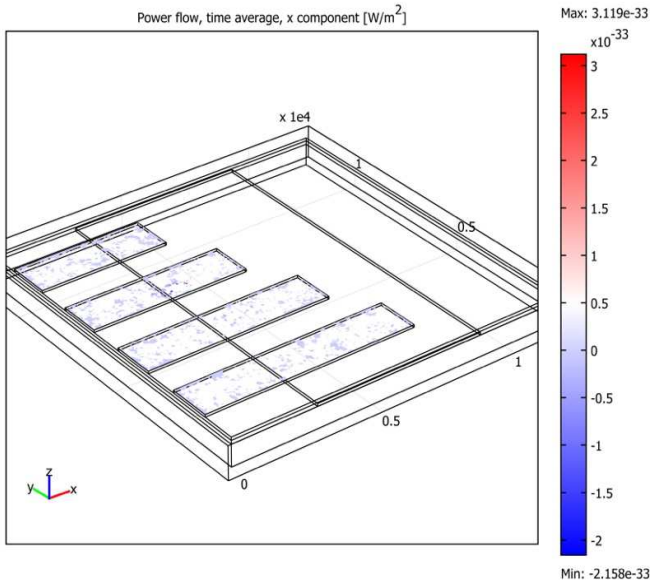

Fig. 8 Power flow, time average, x component [W/m^2] in a device without gold layer.

We have compared the power spectral density for values obtained by simulation model with and without a layer of gold referred to the wavelength range between 400 nm and 800 nm and the electric power values obtained by experimental data for each organic solar cell.

III. Results and Discussion

The device was characterized by measuring of currents and voltages. The measurements were performed under illumination using a solar simulator that produces light with 100 mW/cm^2 to reproduce the sun spectrum (AM 1.5). The IV traces were obtained using the source-measure unit Keithley 2420. The current-voltage characteristics of OSCs with and without a thin film of gold ranging from 0 to 0.7 Volts as shown in Fig. 9.

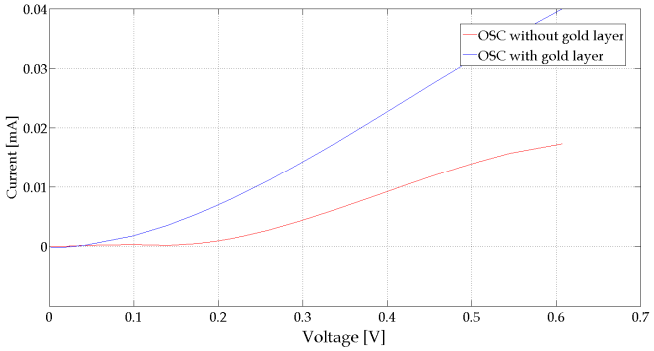

Fig. 9 Current-Voltage (I-V) curves of organic solar cells with and without gold layer.

It is worth noticing that the OSC containing a gold layer exhibited better performances. Fig. 10 shows the electric power extracted by the I-V characteristic of an organic solar cell with length of 5.50 mm in the organic sample (12 mm x 12 mm).

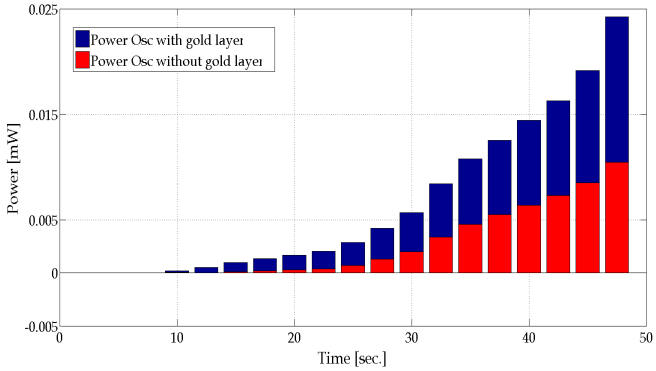

Fig. 10 Electric power obtained by experimental organic devices

The configuration model with layer of gold reaches a maximum electric power peak of 0.0239 mW while the maximum value for Osc without layer of gold is 0.01mW. This latter value is considerably lower, so proving that gold layer increases the efficiency and performance of organic devices.

IV. Conclusions

In this paper, two organic cell models are analyzed: the first exhibiting a gold layer for multilayer structure GLASS/ITO/PEDOT:PSS/P3HT: PCBM and the other organic sample without it. These structures have been implemented and compared with simulated models derived from physical devices. The results and comparison show that the gold layer model has increased the electrical performances with respect of others.

References

[1] L., Safriani, et al. "Charge carrier dynamics of active material solar cell P3HT: ZnO nanoparticles studied by muon spin relaxation (μSR)." *Advanced Materials Research*. Vol. 896, pp. 477-480, Trans Tech Publications Ltd, 2014.

[2] M., Sauki, et al. "The structural and electrical properties of nanostructures ZnO thin films on flexible substrate." *International Journal on Advanced Science, Engineering and Information Technology* . Vol. 7, n. 3, pp. 822-828, (2017).

[3] W. O. S., Arsyad, et al. "Revealing the limiting factors that are responsible for the working performance of quasi-solid state DSSCs using an ionic liquid and organosiloxane-based polymer gel electrolyte." *Ionics*, Vol. 24, n.3, pp. 901-914, (2018).

[4] H. B., Nguyen, and T. A., Bui, "Developing The Solar Tracking System for Trough Solar Concentrator." *International Journal on Advanced Science, Engineering and Information Technology*, Vol. 6, n. 1, pp. 58-60, (2016).

[5] A., Pangdam, et al. "Investigation of gold quantum dot enhanced organic thin film solar cells." *Particle & Particle Systems Characterization*, Vol. 34, n. 11, pp. 1700133, (2017).

[6] G., Lo Sciuto, G., Capizzi, S., Coco, R. , Shikler, "Geometric shape optimization of organic solar cells for efficiency enhancement by neural networks" *Lecture Notes in Mechanical Engineering*, pp. 789-796, (2017), DOI: 10.1007/978-3-319-45781-9_79.

[7] G., Capizzi, G., Lo Sciuto, C., Napoli, R., Shikler, M., Wozniak, " Optimizing the organic solar cell manufacturing process by means of AFM measurements and neural networks", *Energies*, Vol. 11, n. 5, art. no. 1221, (2018), DOI: 10.3390/en11051221.

[8] G., Lo Sciuto, "Application of artificial intelligence for optimizing an organic solar cells production process", *Photonics Letters of Poland*, Vol.12, n.2, pp. 34-36,(2020), DOI: 10.4302/plp.v12i2.993.

[9] G., Lo Sciuto, S., Coco, "A 3D finite element model of degradation phenomena in organic solar devices affected by oxidation", *International Journal of Energy and Environmental Engineering*, Vol.11, n.4, pp. 431-437, (2020), DOI: 10.1007/s40095-020-00345-1.

[10] G., Lo Sciuto, C., Napoli, G., Capizzi, R., Shikler, "Organic solar cells defects detection by means of an elliptical basis neural network and a new feature extraction technique" *Optik*, Vol. 194, art. no. 163038, (2019), DOI: 10.1016/j.ijleo.2019.163038.

[11] D., Subara and , I. Jaswir, "Gold Nanoparticles: Synthesis and application for Halal Authentication in Meat and Meat Products." *International Journal on Advanced Science, Engineering and Information Technology*, Vol. 8, n. 4-2, pp. 1633-1641, (2018),

[12] H., Pujiarti, R., Hidayat and P., Wulandari, "Enhanced efficiency in dye-sensitized solar cell by localized surface plasmon resonance effect of gold nanoparticles." *Journal of Nonlinear Optical Physics & Materials*, Vol. 28, n. 4, pp. 1950040, (2019).

[13] N. S., Suhaimi, et al. "Brea ppkdown strength of transformer oil filled with carbon nanotubes under various gap distances." *Journal of Fundamental and Applied Sciences*, Vol. 9, n. 3S, pp. 41-60, (2017).

[14] M. Diethelm, et al. "Finite element modeling for analysis of electroluminescence and infrared images of thin-film solar cells." *Solar Energy*, Vol. 209, pp. 186-193, (2020).

[15] L. Q., Cao, Z., He, E. I., Wei, and R. S., Chen, "Influence of Geometry of Metallic Nanoparticles on Absorption of Thin-Film Organic Solar Cells: A Critical Examination." *IEEE Access*, Vol. *8*, pp.145950-145959, (2020).

[16] J., Sladek, V., Sladek, M., Repka and S., Schmauder, "Mixed FEM for quantum nanostructured solar cells." *Composite Structures*, Vol. 229, pp. 111460, (2019).

[17] S., Zandi and M., Razaghi, "Finite element simulation of perovskite solar cell: A study on efficiency improvement based on structural and material modification." *Solar Energy*, Vol. 179, pp. 298-306, (2019).

[18] K. W., Seo, J., Lee, J., Jo, C., Cho and J. Y., Lee, "Highly efficient (> 10%) flexible organic solar cells on PEDOT□free and ITO□free transparent electrodes." *Advanced Materials*, Vol. *31*, *n.* 36, pp. 1902447, (2019).

[19] G., Lucarelli and T. M., Brown, "Development of highly bendable transparent window electrodes based on MoOx, SnO2 and Au dielectric/metal/dielectric stacks: application to indium tin oxide (ITO)-free perovskite solar cells." *Frontiers in Materials*, Vol. 6, pp. 310, (2019).

[20] A. Way et al. "Fluorine doped tin oxide as an alternative of indium tin oxide for bottom electrode of semi-transparent organic photovoltaic devices." *AIP Advances*, Vol 9, n. 8, pp. 085220, (2019).